

1 **Discordant population structure inferred from male- and female-**
2 **type mtDNAs from *Limecola balthica*, a bivalve species**
3 **characterized by doubly uniparental inheritance of mitochondria**

4
5 ¹Le Cam Sabrina, ^{1,2}Brémaud Julie, ¹Becquet Vanessa, ¹Huet Valérie, ¹Garcia Pascale,
6 ^{1,3}Viricel Amélie, ²Breton Sophie, ^{1,3}Pante Eric

7
8 ¹Laboratoire Littoral Environnement et Sociétés (LIENSs), UMR 7266 CNRS-LRU, 17000
9 La Rochelle, France

10 ²Département de sciences biologiques, Université de Montréal, Montréal, QC, Canada

11 ³Laboratoire des Sciences de l'Environnement Marin (LEMAR), UMR 6539 CNRS-UBO-
12 IRD-Ifremer, Institut Universitaire Européen de la Mer, 29280 Plouzané, France

13

14 Corresponding author: eric.pante@cnrs.fr

15

16 **Abstract**

17

18 Doubly Uniparental Inheritance (DUI) of mitochondria is a remarkable exception to the
19 Strictly Maternal Inheritance (SMI) in metazoans. In species characterized by DUI --almost
20 exclusively gonochoric bivalve mollusks--, females (F) transmit mitochondria to offspring of
21 both sexes, while males (M) pass on their mitochondria exclusively to their sons. Under DUI,
22 males are heteroplasmic, somatic tissues containing F-transmitted mtDNA and gametic cells
23 containing M-transmitted mtDNAs. The aforementioned transmission routes make M- and F-
24 transmitted mtDNA interesting as sex-specific markers which can differ in their effective
25 population sizes, mutation rates, and selective constraints. For these reasons, looking at both
26 markers can provide significant insight into the genetic structure of populations and
27 investigate its determinants. In this study, we document differences in genetic diversity,
28 divergence, inter-populational genetic differentiation and biogeographic structure between
29 M- and F-type *cox1* mt genes in the Baltic tellin (*Limecola balthica*) to test whether *cox1m*
30 and *cox1f* genes bear the marks of similar phylogeographic histories. Both markers were
31 sequenced for 313 male individuals sampled from the Baltic Sea to the Gironde Estuary
32 (Southern France). Haplotype diversity and net divergence were over twice higher in *cox1m*

33 compared to *coxIf*. A strong southward decrease in nucleotide diversity was observed only at
34 *coxIm*. Genetic differentiation between northern and southern populations was nearly 3 times
35 higher at *coxIm* compared to *coxIf* (global $\Phi_{ST} = 0.447$ and 0.126 respectively) and the
36 geographic localization of the strongest genetic break significantly differed between the
37 markers (Finistère Peninsula at *coxIf*; Cotentin Peninsula at *coxIm*). A higher mutation rate,
38 relaxed negative selective pressure and differences in effective population sizes (depending
39 on locations) at *coxIm* could explain differences in population genetic structure. As both F-
40 and M-type mtDNAs interact with nuclear genes for oxidative phosphorylation and ATP
41 production, geographical discordances in genetic clines could be linked to mito-nuclear
42 genetic incompatibilities in this system.

43

44 **Keywords**

45 Doubly Uniparental Inheritance, disruption, heteroplasmy, comparative biogeography,
46 phylogeography, discordance, hybrid zone, genetic cline, mitochondria

47

48 **Introduction**

49 Some species show a remarkable exception to the maternal inheritance of mitochondria in
50 metazoans: the doubly uniparental mode of inheritance (DUI). In this system, both males and
51 females are able to transmit their mitochondria. The former transmits “female-inherited” (F-
52 type) mitochondria to all their progeny and the latter pass on “male-inherited” (M-type)
53 mitochondria to their male offspring, where the male mitogenomes (mt) are quartered in male
54 germ line and gametes (reviewed in Zouros, 2013). To date, DUI species have only been
55 discovered in the class Bivalvia, with over 100 DUI species (Gusman et al 2016) among the
56 about 11,000 contained in this taxon (Huber 2010, 2015). They are all gonochoric, except for
57 the hermaphroditic mussel *Semimytilus algosus* (Lubosny et al 2020). More than a simple
58 peculiarity, DUI is suspected to play a role in sex-determination and gonad differentiation
59 (Zouros 2000, Breton et al 2011, Guerra et al 2017, Capt et al 2018, 2019), and could well be
60 involved in population structure through intrinsic (*e.g.* genetic incompatibilities; Saavedra et
61 al 1996) and extrinsic (*e.g.* selection and demography, Stewart et al 1996) factors.

62 In DUI species, the divergence between F-type and M-type mitogenomes is variable
63 but generally high, ranging from 6 to over 50% (reviewed in Breton et al 2007 and Gusman et
64 al 2016), which questions the maintenance of mito-nuclear genetic coadaptation. Indeed, both
65 F- and M-type mitochondria can be found in males and females but in majority, females are

66 homoplasmic for the F-type mtDNA whereas males are heteroplasmic, accommodating two
67 highly divergent mitogenomes (F-type in somatic tissues and M-type in sperm). The presence
68 of the M-type mtDNA in somatic tissues is considered as a paternal leak due to elimination or
69 segregation failure of sperm mitochondria in female or male embryos, respectively (Milani et
70 al 2012). Both F- and M-type mt lineages show rapid molecular evolution compared to other
71 animals, the M-type mtDNA usually evolving faster than the F-type mtDNA (Zouros et al
72 2013). Coevolution and coadaptation of mitochondrial and nuclear genes are required for
73 efficient cellular energy production (*i.e.* oxidative phosphorylation OXPHOS) and mito-
74 nuclear genetic incompatibilities (MNIs) can lead to a desynchronization of this machinery
75 (Burton & Baretto 2012,2013). Therefore, DUI offers tremendous potential for genetic
76 incompatibilities to develop, in particular, in inter-populational hybrids, as a network of cyto-
77 nuclear interactions exists (Saavedra et al 1996): mito-genetic incompatibilities can be
78 expressed not only between the F-type and nuclear genes (in somatic tissues and oocytes in
79 females), but also between the M-type and nuclear genes in sperm. Recombination between
80 M- and F-types can further complicate mito-nuclear dynamics (reviewed in Zouros 2013).
81 DUI could, therefore, bear on the maintenance of genetic structure among populations of
82 highly dispersive bivalve species at small spatial scales, and provide key insight into the
83 establishment and maintenance of local adaptation. While significant efforts have been made
84 in the recent years to comprehend how DUI works and how it evolved (*e.g.* Breton et al 2007,
85 2014; Zouros, 2013, Zouros 2020), little information is available on how it might participate
86 to reproductive isolation.

87 Thus, barriers to gene flow can arise and be maintained by a multitude of
88 environmental and/or intrinsic factors (Barberousse et al 2010), from ecological isolation to
89 genetic incompatibilities. Hybrid zones, which correspond to transition regions between
90 spatially separated genetic stocks, are “natural laboratories” to study the interactions between
91 intrinsic barriers and the environment, and the processes of adaptation and speciation.

92 *Limecola balthica* (previously known as *Macoma balthica*, Huber, 2015), a species in
93 which DUI has recently been detected (Pante et al 2017), is a noteworthy model species to
94 study hybrid zones in marine ecosystems (Strelkov et al 2007, Riginos & Cunningham 2007).
95 It has a wide distribution range spanning from the west pacific coasts, in Japan and from
96 Alaska to Oregon (USA, Luttikhuizen, 2003) to the North Atlantic, where the species is
97 found in the west from Arctic to Virginia (USA; Meehan, 1985) and in the east from the
98 north of Russia (Hummel et al, 1997) to the Arcachon Basin (Hily 2013 and this publication).
99 The succession of glaciation and inter-glaciation periods has resulted in colonization events

100 of the Atlantic marked by repeated isolation, invasion, and re-colonization events (Nikula et
101 al, 2007). These episodic colonization events have created multiple opportunities for
102 secondary contacts between different genetic stocks and the establishment of several hybrid
103 zones in the Atlantic. Two subspecies of *L. balthica* co-occur in North Atlantic: a Pacific
104 lineage (*L. balthica balthica*) present in the Baltic Sea and the White Sea, and an Atlantic
105 lineage (*L. balthica rubra*) present in the Norwegian Sea, the North Sea and along the British
106 coasts, down to the southern range limit of the species (Väinölä 2003, Lutikhuisen et al
107 2003, Nikula et al 2008). In Europe, genetic breaks were described in the Kattegat-Detroit
108 between Sweden and Denmark (Nikula et al. 2007, 2008) and in the North Finistère between
109 the Channel and the Atlantic Ocean. Southern populations of *L. balthica rubra* exhibit F-type
110 mtDNA signatures consistent with long-term isolation in the glacial refugium of the Bay of
111 Biscay: high genetic diversity relative to previously-glaciated areas, high prevalence of
112 private alleles, and a sharp genetic break separating them from northern populations (Becquet
113 et al 2012). Multiple genes involved in the oxidative phosphorylation (OXPHOS) system
114 (including genes coding for ATP synthase subunits and an ADP/ATP transporter were
115 detected as significantly differentiated among southern and northern populations by an F_{ST}
116 scan (Pante et al 2012, 2019). These results suggested that incompatibilities between
117 mitochondrial and nuclear genes encoding OXPHOS functions could be involved in
118 endogenous barriers to gene flow in *L. balthica*.

119 Here, we present sharp differences in genetic diversity, divergence and population
120 genetic structure between F- and M-type mtDNAs of *L. balthica* male individuals, in
121 particular along the northeast Atlantic hybrid zone first described in Becquet et al (2012).
122 Given the typically higher evolution rate and the potentially relaxed selection pressures acting
123 on the M-type mitogenome, these comparative data allow us to start testing whether
124 mitotypes are sufficiently different to cause genetic incompatibilities impeding gene flow in
125 *L. balthica*.

126

127 **Materials and Methods**

128

129 **Sampling**

130 Individuals were collected from a total of 17 sampling sites ranging from Arcachon (southern
131 range limit of the species, France) to Le Crotoy (Somme Bay, northern France) and from
132 Kruiningen (the Netherlands) to Umea (Swedish Baltic Sea) (Table S1). Individuals from

133 sampling sites on the French coasts were treated as follows: 70 to 100 adults from 11 mm to
134 23 mm were randomly collected live at sexual maturity between 4th and 23rd of April 2018
135 at 9 locations ranging from the Bay of Biscay in southern France to Somme Bay (Table S1).
136 Individuals were then held in aquaria until dissection at the LIENSs laboratory (LIttoral
137 ENvironnement et Sociétés) in La Rochelle, France, with water temperature maintained at
138 10°C. They were fed with a multispecific microalgal mixture every other day and dead or
139 dying individuals were removed daily if necessary. For each individual, the adductor muscle
140 was carefully severed to separate the two valves, without damaging the gonad, and a sample
141 of the mantle was taken. Sex and gonadal maturation stage were determined with a dissecting
142 microscope (x100 to x400). For each individual, two types tissue samples were collected, a
143 gonadic sample and a somatic sample (mantle). All tissue samples were flashfrozen in liquid
144 nitrogen, and then stored at -80°C until DNA extraction. At each step of this protocol,
145 dissecting tools and bench surfaces were thoroughly cleaned in successive baths of 10 %
146 bleach, demineralized water, and 95 % EtOH as to avoid DNA cross-contamination. Using
147 this dataset, we checked that male mitochondria were limited to male gonads (*i.e.* absent from
148 other male tissues and from females); thus making molecular sexing permissible (Le Cam et
149 al in prep).

150 For the other sampling sites, whole individuals had been collected for a previous
151 study (Becquet et al. 2012 and the BIOCOMBE project) and were preserved in 95% EtOH. A
152 3 mm³ piece of tissue was sampled from the gonad, gDNA was purified and quantified as
153 detailed below, and PCR amplifications were attempted with both the *cox1m* and *cox1f*
154 primers. Individuals for which both gene regions could be amplified were considered as
155 males and included in subsequent analyses.

156

157 **Molecular Analyses**

158 Total DNA was extracted with the Nucleospin Tissue Kit (Macherey Nagel), following the
159 manufacturer's instructions. In Saint-Vaast and Mont Saint Michel, most specimens were
160 sexually undifferentiated at the time of sampling. Therefore, for these samples and for the
161 samples from all the other "non-French" localities, sex was determined by checking for the
162 amplification of both male and female *cox1* markers in gonad DNA. DNA purity and
163 potential contaminants were checked using a NanoDrop2000.

164 Polymerase chain reaction (PCR) amplifications of the female (*cox1f*) and male
165 (*cox1m*) mitochondrial DNA regions were performed using specific primers (Cox1m:
166 *cox1m14641F* ATAGCTGGCCTGGTGTTTAGG, *cox1m15560R*

167 TTGGACCCTTTCGAGCCAAG; Cox1f: *cox1f5343F* TTAGTGACTTCACACGGTTTGC,
168 *cox1f6032R* TGGGAAATAATCCCAAACCCG). Amplifications were realized in a total
169 volume of 25 μL , with 0.1 μL of Taq Polymerase 5 $\text{U}\cdot\mu\text{L}^{-1}$ (TaKaRa Ex Taq® Kit MgCl_2
170 Free Buffer) (TaKaRa Ex Taq, TaKaRa Bio, Shiga, Japan), 2.5 μL PCR Buffer 10X, 1.5 μL
171 MgCl_2 25 mM, 1 μL dNTP 2.5 mM each, 0.6 μL each primer 10 μM and 17.7 Milli-Q water,
172 and 1 to 20 ng of template DNA. SensoQuest thermal cyclers (Göttingen, Germany) were
173 used to perform the following PCR cycling profiles: (i) for the *cox1f*, 2 min of initial
174 denaturation at 94°C, then 30 cycles consisting of 45 sec at 94°C followed by 30 sec of
175 annealing at 57°C and 40 sec of elongation at 72°C, and a 5 min final step of elongation at
176 72°C, and (ii) for the *cox1m*, 2 min at 94°C, then 30 cycles of 30 sec at 94°C, 30 sec at 60°C
177 and 55 sec at 72°C, and a final elongation for 5 min at 72°C. PCR success (*i.e.* amplicon
178 concentration, specificity and absence of amplicons for PCR and extraction negative
179 controls), was tested on 1% agarose gels. PCR products were then sent to Eurofins GATC
180 Biotech GmbH (Konstanz, Germany) to be purified and Sanger sequencing was performed on
181 both directions.

182 **Sequence Analyses**

183 All sequences of *cox1f* sequences and *cox1m* fragments were quality-controlled and aligned
184 in Geneious Prime 10.2.6 (Kearse et al 2012). Consensus sequences were trimmed to 479 bp
185 and 676 bp for *cox1f* and *cox1m*, respectively. Full length *cox1m* (676 bp) was called *cox1m-*
186 *long* hereon and trimmed *cox1m* sequences at the same length as *cox1f* (479bp) to compute
187 further comparative analyses was referred to *cox1m* hereon.

188 Haplotype sequences and their frequencies from *cox1-long* computed in R v3.3.3 (R Core
189 Team, 2017) using the *pegas* package v0.11. (Paradis, 2010) In order to model intraspecific
190 relationships among haplotypes, for both *cox1f* and *cox1m-long*, median-joining networks
191 (Bandelt et al., 1999) were constructed with PopART v1.7 software (Leigh & Bryant, 2015).

192 Genetic diversity indices and population differentiation analyses at *cox1f* and *cox1m*
193 were estimated only for sampling sites with a minimum sample size of 10 individuals.
194 Genetic diversity indices were calculated using Arlequin v3.5.2.2 (Excoffier et al., 1992):
195 haplotype number (H), haplotype diversity (H_d) and nucleotide diversity (π Tajima, 1983).
196 Index distributions were statistically compared using paired non-parametric Mann-Whitney-
197 Wilcoxon tests. Genetic differentiation was estimated in Arlequin using the F_{ST} fixation
198 index and its statistical significance was tested by performing 10,000 permutations (Excoffier
199 et al., 1992).

200 An analysis of molecular variance (AMOVA) was carried out to evaluate the genetic
201 structure among geographic regions and overall sampling sites using 10,000 permutations
202 with Arlequin v3.5.2.2 (Excoffier et al., 1992). We used jModeltest2 (Darriba et al., 2012;
203 Guindon & Gascuel, 2003) to choose the Tamura-Nei model of nucleotide substitution (with
204 gamma shape parameters of 0.1150 and 0.1450 for *coxI*f and *coxI*m respectively) as a
205 measure of haplotype distances in Arlequin. Based on discordances in the distribution of the
206 genetic diversity at *coxI*f and *coxI*m, several hierarchical groupings of subpopulations were
207 tested for each marker to determine the best geographical delineation of genetic structure.

208 Different measures of populations differentiation (pairwise and AMOVA) were also
209 carried out using conventional F- statistics.

210 To test for differences in selective pressure on the female and male mitochondrial sequence
211 sets, the Tajima's D (Tajima, 1989) test for deviations from the neutral theory model for a
212 population of constant size was calculated in Arlequin v3.5.2.2 (Excoffier et al., 1992) for
213 each marker and sampling sites. Its statistical significance was tested with 10,000
214 permutations. The McDonald and Kreitman test (McDonald and Kreitman 1991) was used to
215 compare polymorphism and divergence among female and male mitotypes. The test was
216 conducted in DNAsp (Librado and Rozas 2009) within genetically homogeneous groups at
217 the north and south of the hybrid zone.

218 Because the difference in effective population size (N_e) between males and females is often
219 invoked in the literature as a factor influencing the population genetics of M- and F-
220 mitogenomes, we estimated this parameter using three different methods: first, based on the
221 method used in Ladoukakis et al (2002), the ratio of the male and female genome effective
222 size N_e was estimated based on

223 (i) the expected effective number of alleles under neutrality formulated by Crow and
224 Kimura (1970, equation 7.2.5)

$$225 \quad n_e = CN_e\mu + I \text{ (not } n_e = Cn_e\mu \text{ as written Ladoukakis et al 2002)}$$

226 C being variable according to the mutation model and the genome (mitochondrial vs
227 nuclear). Conversely to Ladoukakis et al 2002, because we estimated a male mitogenome
228 mutation rate (μ_M) twice as high as μ_F , the mutation rate term was μ was kept in the
229 equation:

$$230 \quad \frac{N_{eF}}{N_{eM}} = \frac{n_{eF}-1}{n_{eM}-1} \times \frac{\mu_M}{\mu_F}$$

231 (ii) an estimate of n_e given by Zouros (1979, equation 15)

232
$$n_e = \frac{1}{1-Hd}$$

233

234 This method solely relies on the estimate of haplotype diversity Hd and the mutation rate μ .
235 The marker-specific mutation rates were estimated together with the molecular clocks as
236 described thereafter in the paragraph. Second, π_a/π_s was used as a proxy N_e since small N_e
237 are expected to exhibit a higher segregating mutation load (high π_a/π_s) (Galtier and
238 Rousselle 2020).

239 Last, we used Coalescent Bayesian Skylines to estimate differences in demographic
240 history between the male and the female mitochondrial markers, both sampled from male
241 individuals. This method is based on the tree topology, from which is extracted the rate of
242 coalescent event and hence N_e (Drummond et al 2005). For this, we focused on a southern
243 group composed of Arcachon, Fouras, Aytré and Saint Brévin, and on a northern group
244 composed of Kruiningen, Crildumersiel, Wilhelmshaven and Sylt. In both case, populations
245 are genetically homogeneous (Tables S2 and S3), unambiguously outside of the
246 Finistère/Cotentin hybrid zone. Sample sizes were 102 and 42 males, respectively. First, we
247 estimated a molecular clock for the male and female *cox1* gene by calculating the genetic
248 distance among sequences of *L. balthica* and *Donax*, another Tellinoidea characterized by
249 DUI (Theologidis et al 2008; Gusman et al 2016). For *L. balthica*, we used m and f
250 haplotypes from Umea and Arcachon as extremes on the haplotypes networks (Fig 1). For
251 *Donax*, we used GenBank records for *D. faba* (AB040843 and AB040844 for m and f *cox1*,
252 respectively) and for *D. cuneatus* (AB040841 and AB040842 for m and f *cox1*, respectively).
253 The mean genetic distance (Kimura 2-parameters distance, Kimura 1980) between all
254 *Limecola / Donax* sequence pairs were used to calculate a marker-specific molecular clock,
255 given a divergence time of 90 to 140 My between the two genera (as in Luttikhuisen et al
256 2003, based on fossil dating in Pohlo 1982). To run the Bayesian skyline analysis, we
257 followed the protocol of Müller and du Plessis (Barido-Sottani et al 2018). For each dataset
258 (male and female) and for each extreme of the estimated molecular clocks, we ran BEAST
259 v2.6.3 (Bouckaert et al 2019) using a GTR+G+I site model, a strict clock model, 800M
260 generations with a pre-burnin of 80M generations. The number of dimensions (groups of
261 coalescent events) was set to 3 after test runs with 3 to 5 dimensions. Other priors were left at
262 their default values. Convergence was checked in Tracer v1.7.1. N_e estimates are presented

263 as median values for the retained runs for the low mutation rate, unless otherwise noted.
264 Generation time for *L. balthica* is 2 yrs (Beukema et al 2001).

265

266 **Results**

267 A total of 666 individuals from 17 sampling sites of the French Atlantic coast were dissected
268 and optical microscopy sexing reported 248 males, 185 females and 233 undifferentiated
269 individuals. Undifferentiated specimens might have released their gametes or resorbed them,
270 as lipid droplets were observed in some of the undifferentiated gonads. Molecular sexing was
271 used to detect males in undifferentiated individuals.

272 Both *cox1m-long* and *cox1f* were successfully sequenced for 313 male individuals
273 from 17 sampling sites (Table 1). Sampling size per site ranged from 2 to 33 overall sampling
274 sites and from 28 to 33 when only considering sampling sites in France, apart from Arcachon
275 (N=10). We used *cox1m-long* for haplotype networks (Fig 1) and haplotype geographical
276 frequencies (Fig 2). All other analyses were performed on *cox1m* rather than *cox1m-long* to
277 compare M and F markers in a strict, quantitative fashion.

278 Among the 313 studied individuals, 37 and 81 haplotypes were found for *cox1f* and
279 *cox1m-long*, respectively. Among these, 57% were singletons at *cox1f* and 80% at *cox1m-*
280 *long*. Median joining networks showed a similar geographical pattern with three main
281 haplogroups encompassing mainly the northern, central and southern samples (Fig 1 A and
282 C). A second *cox1m-long* central haplogroup (IIb) containing 6 haplotypes was observed and
283 only found in the hybrid zone (MSM: Mont Saint Michel and BRI: Saint Brieuç).
284 Nonetheless, the networks revealed important differences between markers. First, *cox1m-long*
285 not only presented a higher diversity, but also a higher divergence level: a maximum of 24
286 and 40 mutation steps separated the most divergent haplotypes for *cox1f* and *cox1m-long*,
287 respectively. Haplotype networks and frequencies for the truncated *cox1m* dataset are
288 presented in Fig S1 and revealed similar pattern of high diversity (64 haplotypes) and
289 divergence (9 mutation steps were estimated between the main central haplotype and the
290 northern one for *cox1f* against 18 for *cox1m*). We estimated divergence rates of 0.47 s/s and
291 0.24 s/s for the m and f datasets, respectively. This difference is significant based on the
292 relative-rates test (100% significant comparisons out of 2368
293 <https://github.com/lly005/Relative-Rate-Test>). This resulted in molecular clocks of 0.0033
294 and 0.0017 s/s/My for *cox1m* and *cox1f*, respectively, considering a 140My divergence

295 between *Limecola* and *Donax*; 0.0052 and 0.0027 s/s/My for *cox1m* and *cox1f*, respectively,
296 considering a 90 My divergence between these taxa.

297 The relative frequencies of the haplogroups illustrated in Fig 2 showed different
298 patterns. The *cox1m-long* haplogroup I was present only in Baltic and North Sea samples
299 while the *cox1f* haplogroup I encompassed individuals from the Baltic Sea to the English
300 Channel (hybrid zone). Also, the haplogroup II of *cox1f* was shared among the Baltic Sea,
301 North Sea, the English Channel and Atlantic samples whereas the main central haplogroup
302 (IIa) of *cox1m-long* was found only in the North Sea and the Channel Sea. Interestingly, clear
303 genetic breaks were revealed for each marker and they were not located at the same
304 geographical location. For the *cox1m-long*, the Cotentin peninsula represented a sharp
305 transition zone between the haplogroups IIa and III which was confirmed by pairwise Φ_{ST}
306 values (Table S2). Two homogenous populations were observed north of the Cotentin
307 peninsula and the south of the Finistère (within group pairwise Φ_{ST} ranged from -0.05 to
308 0.04) and these populations were highly differentiated (between group pairwise Φ_{ST} ranged
309 from 0.38 to 0.61). In between, the BRI and MSM sampling sites were very differentiated
310 (between group pairwise Φ_{ST} ranged from 0.50 to 0.61) from the North of the Cotentin but
311 they were also weakly yet significantly different from some sites at the South of the Finistère
312 (between group pairwise Φ_{ST} ranged from 0.02 to 0.04). For *cox1f*, the pattern was more
313 complex. The haplogroup III was composed of haplotypes found in majority at the south of
314 the Finistère (Fig 2) and samples from either side of the Finistère were highly divergent
315 (pairwise Φ_{ST} ranging from 0.41 to 0.79, Table S3). On both sides of the Finistère peninsula,
316 significant population substructure was detectable: the Pont Mahé (MAH) sampling site was
317 mildly differentiated from Saint Brévin (BRE) and Aytré (AYT) (pairwise Φ_{ST} of 0.13 and
318 0.08 respectively, table S3). Also, the relative frequency of the 3 haplogroups was variable in
319 the north of the Finistère peninsula, resulting in a patchy distribution of the genetic diversity
320 (Fig 2). Saint Briec (BRI) for instance was highly differentiated from all other northern sites
321 except from MSM (Mont Saint Michel). Based on these results, genetically homogenous
322 sampling sites were merged in 3 geographical groups presented in Table 1 and used in
323 subsequent analysis (North, Center and South). The hybrid/Finistère group showed genetic
324 differentiation only for *cox1m*.

325 Haplotypes from the extreme haplogroups were rarely shared within one individual
326 (Fig1 B) and while 17 individuals exhibited the haplogroup I at *cox1f* and the haplogroup III
327 at *cox1m*, no individual shared the *cox1f* haplogroup III and the *cox1m* haplogroup I. Also,
328 only 4 individuals presented both the *cox1f* haplogroup III and the *cox1m* haplogroup IIa,

329 suggesting non-random mating or lethal haplotype combinations. Noteworthy, all these
330 individuals were found in the hybrid zone sampling sites. These results were confirmed by
331 the significant linkage disequilibrium test carried out among haplogroups for phased data
332 (T₂ test df=6, p<0.001). The heatmap presented in Figure 3 illustrates the frequency of all
333 the possible haplogroup associations and the associated correlation values.

334 The level of genetic diversity also differed between the two markers (Table 1). While
335 the average nucleotide diversity (π) and its range across sampling sites were similar (a mean
336 value of 0.055 and a range of 0 to 0.0141 for *cox1f*; a mean of 0.0038 and a range 0.0004 to
337 0.025 for *cox1m*), the median values of the nucleotide diversity (0.61 and 0.20 for *cox1f* and
338 *cox1m* respectively) showed that the nucleotide diversity is significantly greater for *cox1f*
339 than for *cox1m* (Wilcoxon rank test V= 65 p= 0.002). We observed the lowest nucleotide
340 diversities in southern sampling sites for *cox1m* compared to *cox1f*. The haplotype diversity
341 was not significantly different between the two markers (Wilcoxon rank test, V = 35, p =
342 0.89) but the haplotype diversity showed a significant negative southward trend (a = -0.07,
343 R²= 0.72) only for *cox1m*. Finally, Tajima's D also differed among the two markers. When
344 considering the three geographical groups, significant negative values were found only for
345 *cox1m* indicating the possibility of population expansion after a bottleneck event or selective
346 sweep. For *cox1f*, on the other hand, no sign of deviation from neutral expectations was
347 detected at the population level.

348 Consistently with the haplotype networks, the results of the AMOVAs suggested
349 different geographic structuration patterns for *cox1m* and *cox1f* (Table 2). The best
350 hierarchical model based on the F_{SC}/F_{CT} ratio (least variation within and highest between
351 groups) was different for the two markers: for *cox1f* the best model was two groups separated
352 by the Finistère peninsula (KRU, CRI, CRO, VAA, MSM, BRI vs MAH, BRE, AYT, FOU,
353 ARC) whereas for *cox1m*, the best model was also two groups of subpopulation but with the
354 Cotentin peninsula as a major geographical break (KRU, CRI, CRO, VAA) vs (MSM, BRI,
355 MAH, BRE, AYT, FOU, ARC). The result of the AMOVAs (Table 2) showed similar level
356 of among subpopulation genetic variation relative to the total variation for both markers
357 (*cox1m*: 42% and Φ_{ST} = 0.58, p<0.001; *cox1f*: 44% and Φ_{ST} = 0.55, p<0.001). The level of
358 differentiation among groups was higher for *cox1m* compared to *cox1f* (Φ_{CT} = 0.57, p<0.001
359 and Φ_{CT} = 0.49, p<0.001 for *cox1m* and *cox1f* respectively). Finally, within group genetic
360 structure is detected only for *cox1f* (Φ_{SC} = 0.01, p=0.062 and Φ_{SC} = 0.13, p<0.001 for *cox1m*

361 and *coxIf* respectively). Genetic differentiation analyses based only on haplotype frequencies
362 (conventional F-statistics) were also carried out and gave similar results (not shown).

363 McDonald and Kreitman tests were carried out in two genetically homogeneous
364 groups for both markers: “North” and “South” composed of individuals from KRU, SYL,
365 WIL and CRI sampling sites and from AYT, ARC, BRE and FOU respectively (Table 3). In
366 both groups, the MK tests revealed that the divergence between male- and female-type *coxI*
367 gene showed a significant departure from neutral expectations with a large excess of fixed
368 non-synonymous mutations (Table 3). Also, the very low π_a/π_s within each mitotype in both
369 genetic groups showed that the two genes (*coxIm* and *coxIf*) are under strong purifying
370 selection. Non-synonymous nucleotide diversity in *coxIm* was slightly higher than in *coxIf* in
371 the North group and overall samples but not significantly, suggesting selection pressure
372 acting on *coxI* gene was similar among mitotypes.

373 Two of the three methods used to infer effective population size converged to suggest
374 that contemporary N_{eM} is higher than N_{eF} at northern sampling sites, while the opposite holds
375 at southern sites (Zouros N_{eF}/N_{eM} ratio, Table 1; Bayesian Skyline Plot, Figure 4).
376 Contemporary N_{eF}/N_{eM} calculated using Zouros’ method and BSP at time=0 were 0.91 and
377 0.27 within the northern group and 5.09 and 1.07 within the southern group, respectively
378 (0.13 and 1.09 for high mutation rates, Figure S2). π_a/π_s estimates, on the other hand, were
379 always higher for *coxIm*, suggesting a smaller N_e for this marker compared to *coxIf*
380 regardless of the group considered.

381 BSP further suggested that historical N_e dynamics differed between markers (Figure 4
382 for the high mutation rate and figure S2 for the low mutation rate). Southern populations
383 exhibited N_e ranging between 1 and 4.5 M individuals with similar median values (2.3 and
384 2.5 M for *coxIm* and *coxIf*, respectively), with similar population growth that started about
385 200,000 years ago for *coxIf* (about 122,000 years ago based on the fastest mutation rate).
386 ESS values for the estimated parameters are excellent for the southern group (e.g. posterior
387 ESS between 270 and 422). Northern M-type and F-type datasets exhibited significantly
388 different patterns, with similar N_e for *coxIf* and *coxIm* prior to about 155,600 years ago
389 (about 107,300 for the highest mutation rate), followed by an exponential N_e increase for
390 *coxIm* only. ESS for the posterior were lower than for the southern group, but acceptable
391 (110 to 154).

392

393 **Discussion**

394

395 Investigating genetic structure of the DUI species *Limecola balthica* across a hybrid
396 zone in the English Channel revealed discordant phylogeographic patterns for the female- and
397 male-type mitochondrial *cox1* gene. Because F- and M- mtDNA were compared among
398 homologous regions within heteroplasmic males, variability can be strictly attributed to
399 heredity rather than inter-individual or inter-genic differences. This variability resides in (1) a
400 latitudinal gradient in haplotypic diversity for *cox1m* but not *cox1f*, (2) sharper deviation from
401 neutral expectations of nucleotide diversity levels for *cox1m* relative to *cox1f* that can be
402 attributed to historical demographic changes and / or relaxed purifying selection at the former
403 locus, and (3) discordant geographic clines for M- and F- mtDNAs. Below we discuss these
404 differences considering neutral and selective processes that may have caused them.

405

406 **Genetic diversity: differential latitudinal variation between m and f genes**

407 Male-type mtDNA was almost up to twice as polymorphic as its female counterpart,
408 with more haplotypes, more haplotypes represented by a single male and more segregating
409 sites. Higher polymorphism in the M-type mtDNA, both within and between species
410 (Skibinski et al 1999), is a common feature among DUI species, as reported in *Polittapes*
411 *rhombooides* (Chacon et al 2020), *Pyganodon grandis* (Krebs 2004) and *Mytilus sp.* (Ort and
412 Pogson 2003; Smietanka et al 2009, 2013, 2017). Higher frequency of rare M-type
413 haplotypes (80% of singletons compared to 57% among F-type haplotypes in *L. balthica*) is
414 another largely shared feature among DUI species (Chacon et al 2020, Ort & Pogson 2007,
415 Smietanka et al 2009, 2013, 2017). Major determinants of genetic diversity in animals are
416 linked selection, mutation and effective population size (Ellegren and Galtier 2016). In DUI
417 bivalves, polymorphism might result from different selection pressures on male- and female-
418 type mitogenomes (e.g. Milani et al 2012): female-type mitochondria ensure proper
419 mitochondrial function at the scale of the individual whereas male-type mitochondria, which
420 solely co-occurs in heteroplasmic individuals with the F-type mitochondria (Skibinski et al
421 1994 and Zouros et al. 1994) have to effectively function exclusively in the male germ line
422 and gametes (different ‘arenas of selection’ *sensu* Stewart et al 1996). According to the male-
423 driven evolution hypothesis, higher germ cell divisions in males (Shimmin et al 1993) could
424 result in an enhanced replication rate of the M-type mitochondria during spermatogenesis,
425 providing more opportunities for mutations to accumulate (Rawson and Hilbish 1995 and
426 Stewart et al 1995). In addition, oxidative damage might be important in sperm (Zouros
427 2013), and/or selection pressures on chaperonins and DNA repair genes might be relaxed. We

428 can also expect sex-linked demographic differences to influence polymorphism, if the
429 effective population size differs between males and females; this is supported by our dataset
430 to a large extent at historical (*e.g.* past expansion inferred for *cox1m* in the north) and
431 contemporary time scales. Most hypotheses on the role of selection, mutation and effective
432 population size in shaping genetic diversity in DUI bivalves remain to be empirically tested.

433 However, counter examples do exist. For instance, Beauchamp et al (2020) found
434 more F-type haplotypes than M-type haplotypes in *Pyganodon grandis* (11 and 7,
435 respectively) and *P. lacustris* (20 and 6, respectively). Smietanka et al 2013 (87 F- and 76 M-
436 type haplotypes in *Mytilus trossulus*) and Riginos et al 2004 (132 F- and 56 M-type
437 haplotypes in *Mytilus edulis*) reported the same pattern, although the latter results might be
438 due to the difficulty of amplifying the male-type mtDNA.

439

440 Although often presented as such in the literature, higher polymorphism in males is
441 therefore not a universal feature of the population genetics of DUI species. When genetic
442 diversity was measured using nucleotide diversity π , the two markers differed significantly
443 along the geographical area sampled with a significant positive trend observed between π and
444 latitude at the M-type marker. While it varied between sites, π at *cox1f* displayed no
445 geographic pattern.

446 Estimating π at *cox1f*, regardless of individual sexes, Becquet et al (2012) found that
447 Southern populations, near the species range limit (brought here to Arcachon Basin), were
448 more diverse than northern populations both at mitochondrial and nuclear markers. This
449 pattern was attributed to phylogeography, the Bay of Biscay being a glacial refugium for
450 other species (*eg.* Hewitt 1999; Gomez and Lunt 2007). Contrasting diversity patterns
451 between F-type and M-type mtDNA observed in the present study bear similarities with
452 predictions of population characteristics at the border of the species range (Holt et al 2003,
453 reviewed in Dawson et al 2010). Predictions associated with the hypothesis of genetic
454 impoverishment (H1: few northern migrants enter southern peripheral populations) are
455 mostly met at *cox1m*, while the migration load hypothesis (H2: northern migrants bear alleles
456 that are maladaptive in southern environments) seems to better fit the *cox1f* dataset. Gene
457 flow between populations towards the range limit should be lower under H1 and higher under
458 H2. While populations across the Cotentin were more differentiated at *cox1m* than
459 populations across the Finistère at *cox1f*, Pairwise Φ_{ST} were higher between southern
460 populations at *cox1f* than *cox1m*. Genetic diversity should be low (decreasing toward the

461 range limit) under H1 and high under H2, which is met for *cox1m* and *cox1f*, respectively.
462 These patterns support the hypothesis that different selection pressures act on M-type and F-
463 type mt genes, and therefore on male gametes vs. male adults and female at all life stages.
464 This seems plausible (and testable) if we consider that genetic impoverishment occurs at
465 early life stages in males (gamete and/or early zygote survival) and migration load occurs at
466 all stages, such as was previously hypothesized for mitochondrial function (Pante et al 2012,
467 2019).

468

469 **Discordance of geographic breaks between sex-specific mitogenomes**

470 Both male and female mtDNAs displayed significant segregation of haplotypes in
471 space. As previously described by Becquet et al (2012), southern populations were
472 significantly differentiated from northern ones based on *cox1f*, and a geographical break
473 between these two groups was observed at the Finistère peninsula. Sampling done for the
474 present study narrows the gap between northern and southern populations by about 50 km
475 thanks to the addition of the site of Saint Brieuc Bay, however we failed at sampling any
476 large population between the latter and Pont Mahé, south of Finistère (Fig 2). While
477 anecdotal data support the presence of *L. balthica* near Brest (on the banks of Le Faou River;
478 Hily 2013), we speculate based on field observations (Becquet et al 2012, Le Mao et al 2020
479 and this study) that the Finistère intertidal seem largely inhospitable to this species due to the
480 scarcity of mud flats. It therefore appears as a credible physical barrier to genetic
481 connectivity, and it has been indeed identified in the past as a genetic transition zone for other
482 marine benthic-pelagic species confined to estuaries and bays (muddy-fine sediment species
483 Jolly et al 2005, 2006).

484 Likewise, *cox1m* haplotypes strongly segregated in space, separating southern and
485 northern populations at the Cotentin peninsula. This peninsula is located about 50 km farther
486 East of the Finistère peninsula. As for the Finistère, sandy mud flats hospitable to *L. balthica*
487 are scarce, and our field surveys failed at identifying populations between Mont-Saint-Michel
488 Bay and Saint Vaast, although anecdotal presence of the species was recorded farther along
489 the Cotentin coast and was reported to be present but rare on the Normand-Breton Gulf (Le
490 Mao et al 2020). Along with the scarcity of seemingly appropriate habitat and patchiness of
491 small populations in the intertidal zone of Cotentin, we observed significant differences in
492 gonadal development and spawning phenology between populations on either side of the
493 peninsula. While individuals with full gonads and well-developed gametes were sampled
494 between the 4th and the 23rd of April 2018 from Fouras to Mont Saint-Michel Bay (some

495 individuals having even spawned in the field at MSM and Saint Brieuç), gonads from Saint
496 Vaast and Somme Bay individuals were still in early stages of development by April 19, 2018
497 (most gametes being still undifferentiated). These observations were on par with previous
498 reports suggesting spawning asynchrony across the Cotentin Peninsula, with spawning
499 occurring in early April in Aytré (Saunier 2015) and August in Somme Bay (Ruellet 2013).
500 In the great scallop, *Pecten maximus*, different spawning phenologies were described across
501 the Cotentin peninsula (Lubet et al 1995). As for the Finistère, the Cotentin Peninsula was
502 previously identified as a barrier to gene flow (Jolly et al 2005, Quéméré et al 2016, Handal
503 et al 2020). It is also the southern biogeographical boundary of the northern cold temperate
504 Boreal region (Dinter 2001) with distinct hydrologic and oceanographic features from the
505 western part of the English Channel (Dauvin 2012)

506

507 There are, therefore, multiple exogenous (habitat availability; oceanographic currents,
508 *e.g.* Hily 2013, Dupont et al 2007, Fievet et al 2007) and endogenous (asynchrony in
509 reproductive phenology and genetic incompatibilities, discussed below) barriers that could
510 contribute to the genetic differentiation of populations across these two peninsulas. Whether
511 these breaks are involved in primary intergradation or secondary contact (by geographically
512 stabilizing endogenous genetic barriers; Bierne et al 2011) remains to be answered (we
513 attempted to test scenario of isolation with migration using the present dataset without
514 success). We can nevertheless note that divergence of populations on either side of the
515 Finistère-Cotentin break occurred between 0.11 to 2.6 Myr ago (Luttikhuisen et al 2003),
516 while population expansion on either side of the break took place 107 to 200 k years ago
517 (depending on the marker and on the clock; table 1, Figures 4, S2). We can therefore
518 tentatively speculate that these populations diverged during the penultimate glacial maximum
519 occurring in the NE Atlantic 140,000 years ago (Martin-Garcia 2019) and expanded with
520 secondary contact after that event.

521 The fact that each of these barriers is sex-specific is quite original for a marine
522 invertebrate. In the DUI literature, studies have reported that genetic differentiation across
523 populations is stronger for M-type mtDNA than for F-type mtDNA (Liu et al 1996, Skibinski
524 et al 1999, Riginos et al 2004), and some authors reported discordant genetic structure
525 between markers. The freshwater mussels *Lampsilis siliquoidea* displayed population genetic
526 structure at *cox1f* but none at *cox1m* (Krebs et al 2013). Conversely, Riginos et al (2004)
527 found weak connectivity at F-type mtDNA but none at M-type mtDNA in *Mytilus edulis*
528 across the Atlantic Ocean. At the entrance of the Baltic, rampant introgression of *M. edulis* F-

529 type mtDNA was observed, compared to a sharp cline at M-type mtDNA concordant with
530 M7 lysin (a nuclear gene involved in fertilization; Stukas et al 2009). This makes the
531 population structure described here for *L. balthica* noteworthy in the sense that the
532 phylogeography of F- and M-type mt markers do not simply differ in amplitude or resolution
533 (due to significant differences in mutation rates, μ_M being about twice μ_F) but differ in the
534 geographical position of the haplotypic cline separating southern and northern *L. balthica*
535 *rubra*.

536 While a genetic break located around the Finistère peninsula corresponds to previous
537 results by Becquet et al (2012) for *cox1f* and eight nuclear microsatellites, the Cotentin was
538 not detected as a barrier in that study. However, spatial structure was detected at the nuclear
539 *atp5c1* gene (encoding the gamma subunit of the FO/F1 ATP synthase protein complex)
540 between Mont-Saint-Michel and Somme Bay (Saunier 2015). Non-synonymous point
541 mutations separating southern and northern populations are located in an inter-peptide
542 interaction domain of the gamma subunit, suggesting mito-nuclear incompatibilities (Pante et
543 al 2019). The concordance of *atp5c1* and *cox1m* call for further investigation of
544 incompatibilities involving the male mitogenome specifically.

545 Interestingly, significant differentiation with *cox1f* was detected between Pont Mahé
546 (MAH) and the Saint Brévin (BRE) and Ayré (AYT) populations (Table S3). These two
547 groups, separated by the Vilaine River, were identified as significantly differentiated based
548 on microsatellites, but not *cox1f* in the study of Becquet et al (2012), which was based on
549 individuals from both sexes, while our study focused on males exclusively. We may therefore
550 benefit from higher statistical power to detect differences in differentiation across the Vilaine
551 River. This implies that genetic structure among males at *cox1f* is higher than in females.
552 Although we did not include females in our study, we did compare pairwise ϕ_{ST} values
553 between sampling sites that were common between our study and Becquet's. F_{ST} and ϕ_{ST}
554 were both significantly higher in the dataset composed of males exclusively, compared to the
555 dataset composed of males and females (Figure 5). This pattern can be attributed to stochastic
556 genetic variation (effects of mutations and drift) and/or differences of gene flow between
557 sexes. The geographical discordance observed at the Finistère and Cotentin peninsulas for
558 *cox1f* and *cox1m* are also reminiscent of sex-level differences. Indeed, in studies using
559 female-transmitted mtDNA and male-transmitted Y chromosome to investigate population
560 structure, sex-biased asymmetries are often cited as a determinant of discordant geographic
561 patterns (e.g. Boissinot et al 1997, Trejo-Salazar et al 2021). Sex-level differences in gene
562 flow are scarcely reported but exist in bivalves, as in the protandrous pearl oyster *Pinctada*

563 *mazatlanica*, which effective sex-ratio is strongly biased towards males (Arnaud-Haond et al
564 2003).

565 Interestingly, the *cox1m* IIb haplogroup, branching from the southern haplogroup III,
566 is private to the two populations sampled between Finistère and Cotentin (Saint Brieuc and
567 Mont-Saint-Michel; Figs 1-2). This suggests genetic isolation of these populations and
568 subsequent retention of these private haplotypes in the Gulf. This pattern supports a
569 (re)colonization scenario from the south to the Gulf (fitting “concordant” simulated networks
570 for colonization from a refugium; Maggs et al 2008). An alternative scenario, unsupported by
571 the genetic diversity observed in the south, is a stepwise colonization of the south from the
572 north and the loss of IIb haplotypes in the south either from drift or selection.

573 Other factors could explain the M- vs. F-mtDNA discordance, such as mtDNA
574 introgression and heterogeneity in its rate, hybrid zone movement and drift (Barton and
575 Hewitt 1985, Bierne et al 2003, Toews et al 2012). Patterns of asymmetric introgression of
576 alleles are commonly observed in hybrid zones (Barton and Hewitt 1985) and were observed
577 in the Bay of Biscay between *Mytilus edulis* and *M. galloprovincialis* (Rawson and Hilbish
578 1998). In *L. balthica*, asymmetrical gene flow from North to South was detected at *cox1f*
579 (Becquet et al 2012, this study), and *atp5c1* (Saunier 2015, Pante et al 2019). At that same
580 locus, Gagnaire et al (2012), looking at divergence and selection among populations of the
581 eels *Anguilla rostrata* and *A. anguilla* (two hybridizing sister species) also found evidence of
582 unidirectional introgression from the former to the later. At *cox1m*, little introgression was
583 detectable in *L. balthica*, but nevertheless sensibly higher from north to south.

584 Hybrid zone movement has been recognized for long, as a manifestation of variation
585 in population density, dispersal rate, individual fitness, effects of allele frequencies on
586 population structure, and spatially- or frequency-dependent selection (Barton and Hewitt
587 1985). It has been proposed that the northeastern Atlantic *Mytilus* hybrid zones move parallel
588 to warming sea surface temperatures (Hilbish et al 2012). While a similar phenomenon may
589 occur in Baltic tellins, suggesting that genotype-environment correlations could affect cline
590 geography (Ducos et al unpublished), neutral forces may be sufficient to result in discordant
591 M-type and F-type mtDNA cline centers and width. Indeed, as detailed above, both the
592 Finistère and the Cotentin peninsulas are characterized by low population densities and
593 oceanic currents disrupting along-coast dispersal. While mitochondrial recombination is
594 expected to be rare (or at least, rarely transmitted to offspring; Passamonti et al 2003),
595 looking at whole mitogenomes as well as nuclear genes of mitochondrial function vs. other

596 (putatively neutral) nuclear markers may help shed light on the degree to which the patterns
597 detected at *cox1* and *atp5c1* depart from neutral expectations.

598

599 Whether the asymmetric, discordant clines in *L. balthica* observed here are due to
600 cline movement, differential gene flow, population structure, or selection (Barton and Hewitt
601 1985) remains a fascinating avenue for future research. In particular, introgression across the
602 hybrid zone in the English Channel calls for a test of asymmetric fitness of inter-lineage
603 crosses (e.g., Turelli et al 2007). An involvement of mito-nuclear incompatibilities could
604 explain the observed asymmetric allele frequencies if northern hybrids with southern
605 mitochondria are less fit than southern hybrids with northern mitochondria.

606

607 **Data Accessibility**

608 *Cox1f* and *cox1-long* sequences were submitted to Genbank (accession N° OM855617 -
609 OM855929 and OM856027 - OM856339 respectively). Rcode is available at
610 https://github.com/SabLeCam/Cox1_DUI.

611

612 **Acknowledgements**

613

614 The authors thank Mélanie Rocroy, Patrick Triplet, Thierry Ruellet, Rolet Céline
615 (Association GEMEL, Picardie), Anthony STURBOIS (RNN Baie de Saint-Brieuc,
616 VivArmor Nature) and Xavier de Montaudouin (Station Marine d'Arcachon, UMR 5805
617 EPOC, Université de Bordeaux/CNRS) for their help with sample collection. This work was
618 funded by the ANR (DRIVE project, grant n. ANR-18-CE02-0004-01) and by the contrat de
619 plan Etat-Région (CPER/FEDER) ECONAT (RPC DYPOMAR). We thank the participants
620 of the Biocombe project (“The impact of BIODiversity changes in COastal Marine Benthic
621 Ecosystems;” contract n. EVK3-CT-2002-00072; Research n. OND1290723). Lab work was
622 performed at the Molecular Core Facility at the University of La Rochelle. We thank the
623 bioinformatics platform Toulouse Midi-Pyrénées (Bioinfo GenoToul).

624

625 **References**

626

- 627 [1] S. Arnaud-Haond, M. Monteforte, F. Blanc, and F. Bonhomme. Evidence for male-biased
628 effective sex ratio and recent step-by-step colonization in the bivalve *Pinctada*
629 *mazatlanica*. *Journal of Evolutionary Biology*, 16(5):790–796, 2003.
- 630 [2] H. Bandelt, P. Forster, and A. Rohlf. Median-joining networks for inferring intraspecific
631 phylogenies. *Molecular Biology and Evolution*, 16:37–48, 1999.
- 632 [3] A. Barberousse, N. Bierne, J. Britton-Davidian, P. Cappy, Y. Desdevises, T. Giraud, E.
633 Joussetin, C. Moulia, V. Ravigné, C. Smadja, and S. Samadi. Chapitre 4. La spéciation
634 (dir. Ravigné, V). In F. Thomas, T. Lefevre, and M. Raymond, editors, *Biologie*
635 *Evolutionne*. De Boeck Supérieur, 2010.
- 636 [4] J. Barido-Sottani, V. Boskov a, L. du Plessis, D. Ku hner, C. Magnus, V. Mitov, N. F.
637 Müller, J. Pecerska, D. A. Rasmussen, C. Zhang, A. J. Drummond, T. A. Heath, O. G.
638 Pybus, T. G. Vaughan, and T. Stadler. Taming the BEAST – A community teaching
639 material resource for BEAST 2. *Systematic Biology*, 67(1):170–174, 2018.
- 640 [5] N. Barton and G. Hewitt. Analysis of hybrid zones. *Annual Review of Ecology and*
641 *Systematics*, 16:113– 148, 1985.
- 642 [6] K. C. Beauchamp, T. W. Beyett, M. W. Scott, and D. T. Zanatta. Detection of hybrid
643 *Pyganodon grandis* and *P. lacustris* (Bivalvia: Unionidae) using F-and M-type
644 mitochondrial DNA sequences and geometric morphometrics. *Journal of Molluscan*
645 *Studies*, 86(3):233–239, 2020.
- 646 [7] V. Becquet, B. Simon-Bouhet, E. Pante, H. Hummel, and P. Garcia. Glacial refugium
647 versus range limit: conservation genetics of *Macoma balthica*, a key species in the Bay
648 of Biscay (France). *Journal of Experimental Marine Biology and Ecology*, 432:73–82,
649 2012.
- 650 [8] J. J. Beukema, J. Drent, and P. J. C. Honkoop. Maximizing lifetime egg production in a
651 Wadden Sea population of the tellinid bivalve *Macoma balthica*: a trade-off between
652 immediate and future reproductive outputs. *Marine Ecology Progress Series*, 209(119-
653 129), 2001.
- 654 [9] N. Bierne, P. Borsa, C. Daguin, D. Jollivet, F. Viard, F. Bonhomme, and P. David.
655 Introgression patterns in the mosaic hybrid zone between *Mytilus edulis* and *M.*
656 *galloprovincialis*. *Molecular Ecology*, 12:447–461, 2003.

- 657 [10] N. Bierne, J. Welch, E. Loire, F. Bonhomme, and P. David. The coupling hypothesis:
658 why genome scans may fail to map local adaptation genes. *Molecular Ecology*, 20:2044–
659 2072, 2011.
- 660 [11] S. Boissinot and P. Boursot. Discordant phylogeographic patterns between the Y
661 chromosome and mitochondrial DNA in the house mouse: selection on the Y
662 chromosome? *Genetics*, 146(3):1019–1034, 1997.
- 663 [12] R. Bouckaert, T. G. Vaughan, J. Barido-Sottani, S. Duchêne, M. Fourment, A.
664 Gavryushkina, J. Heled, G. Jones, D. Kuhnert, N. D. Maio, M. Matschiner, F. K.
665 Mendes, N. F. Müller, H. A. Ogilvie, L. du Plessis, A. Popinga, A. Rambaut, D.
666 Rasmussen, I. Siveroni, M. A. Suchard, C.-H. Wu, D. Xie, C. Zhang, T. Stadler, and A.
667 J. Drummond. BEAST 2.5: An advanced software platform for Bayesian evolutionary
668 analysis. *PLOS Computational Biology*, 15(4):e1006650, 2019.
- 669 [13] S. Breton, H. D. Beaupre, D. T. Stewart, W. R. Hoeh, and P. U. Blier. The unusual
670 system of doubly uniparental inheritance of mtDNA: isn't one enough? *Trends in*
671 *Genetics*, 23(9):465–474, 2007.
- 672 [14] S. Breton, D. T. Stewart, S. Shepardson, R. J. Trdan, A. E. Bogan, E. G. Chapman, A. J.
673 Ruminas, H. Piontkivska, and W. R. Hoeh. Novel Protein Genes in Animal mtDNA: A
674 New Sex Determination System in Freshwater Mussels (Bivalvia: Unionoida)?
675 *Molecular Biology and Evolution*, 28(5):1645–1659, 2011.
- 676 [15] R. S. Burton and F. S. Barreto. A disproportionate role for mtDNA in Dobzhansky–
677 Muller incompatibilities? *Molecular Ecology*, 21(20):4942–4957, 2012.
- 678 [16] R. S. Burton, R. J. Pereira, and F. S. Barreto. Cytonuclear genomic interactions and
679 hybrid breakdown. *Annual Review of Ecology, Evolution, and Systematics*, 44:281–302,
680 2013.
- 681 [17] C. Capt, S. Renaut, F. Ghiselli, L. Milani, N. A. Johnson, B. E. Sietman, D. T. Stewart,
682 and S. Breton. Deciphering the Link between Doubly Uniparental Inheritance of mtDNA
683 and Sex Determination in Bivalves: Clues from Comparative Transcriptomics. *Genome*
684 *Biology and Evolution*, 10(2):577–590, 2018.
- 685 [18] C. Capt, S. Renaut, D. T. Stewart, N. A. Johnson, and S. Breton. Putative mitochondrial
686 sex determination in the Bivalvia: insights from a hybrid transcriptome assembly in
687 freshwater mussels. *Frontiers in genetics*, 10:840, 2019.
- 688 [19] G. M. Chacón, A. Arias-Pérez, R. Freire, L. Martínez, S. Nòvoa, H. Naveira, and A.
689 Insua. Evidence of doubly uniparental inheritance of the mitochondrial DNA in
690 *Polittapes rhomboides* (Bivalvia, Veneridae): Evolutionary and population genetic

- 691 analysis of F and M mitotypes. *Journal of Zoological Systematics and Evolutionary*
692 *Research*, 58(2):541–560, 2020.
- 693 [20] J. F. Crow. An introduction to population genetics theory. Scientific Publishers, 2017.
- 694 [21] D. Darriba, G. Taboada, R. Doallo, and D. Posada. jModelTest 2: more models, new
695 heuristics and parallel computing. *Nature Methods*, 9(8):772, 2012.
- 696 [22] J.-C. Dauvin. Are the eastern and western basins of the English Channel two separate
697 ecosystems? *Marine Pollution Bulletin*, 64(3):463–471, 2012.
- 698 [23] M. N. Dawson, R. K. Grosberg, Y. E. Stuart, and E. Sanford. Population genetic analysis
699 of a recent range expansion: mechanisms regulating the poleward range limit in the
700 volcano barnacle *Tetraclita rubescens*. *Molecular ecology*, 19(8):1585–1605, 2010.
- 701 [24] W. P. Dinter. Biogeography of the OSPAR maritime area. Bonn, Germany: Federal
702 Agency for Nature Conservation, 167, 2001.
- 703 [25] A. J. Drummond, A. Rambaut, B. Shapiro, and O. G. Pybus. Bayesian Coalescent
704 Inference of Past Population Dynamics from Molecular Sequences. *Molecular Biology*
705 *and Evolution*, 22(5):1185–1192, 2005.
- 706 [26] L. Dupont, C. Ellien, and F. Viard. Limits to gene flow in the slipper limpet *Crepidula*
707 *fornicata* as revealed by microsatellite data and a larval dispersal model. *Marine Ecology*
708 *Progress Series*, 349:125– 138, 2007.
- 709 [27] H. Ellegren and N. Galtier. Determinants of genetic diversity. *Nature Reviews Genetics*,
710 17(7):422–433, 2016.
- 711 [28] L. Excoffier, P. E. Smouse, and J. M. Quattro. Analysis of molecular variance inferred
712 from metric distances among DNA haplotypes: application to human mitochondrial
713 DNA restriction data. *Genetics*, 131:479–491, 1992.
- 714 [29] V. Fievet, P. Touzet, J.-F. Arnaud, and J. Cuguen. Spatial analysis of nuclear and
715 cytoplasmic DNA diversity in wild sea beet (*Beta vulgaris ssp. maritima*) populations:
716 do marine currents shape the genetic structure? *Molecular Ecology*, 16(9):1847–1864,
717 2007.
- 718 [30] P.-A. Gagnaire, E. Normandeau, and L. Bernatchez. Comparative genomics reveals
719 adaptive protein evolution and a possible cytonuclear incompatibility between European
720 and American eels. *Molecular Biology and Evolution*, 29(10):2909–2919, 2012.
- 721 [31] N. Galtier and M. Rousselle. How much does N_e vary among species? *Genetics*,
722 216(2):559–572, 2020.

- 723 [32] A. Gómez and D. H. Lunt. Refugia within refugia: patterns of phylogeographic
724 concordance in the Iberian Peninsula. In *Phylogeography of southern European refugia*,
725 pages 155–188. Springer, 2007.
- 726 [33] D. Guerra, F. Plazzi, D. T. Stewart, A. E. Bogan, W. R. Hoeh, and S. Breton. Evolution
727 of sex-dependent mtDNA transmission in freshwater mussels (Bivalvia: Unionida).
728 *Scientific Reports*, 7(1):1–13, 2017.
- 729 [34] S. Guindon and O. A. Gascuel. A simple, fast, and accurate algorithm to estimate large
730 phylogenies by maximum likelihood. *Systematic Biology*, 52(5):696–704, 2003.
- 731 [35] A. Gusman, S. Lecomte, D. T. Stewart, M. Passamonti, and S. Breton. Pursuing the
732 quest for better understanding the taxonomic distribution of the system of doubly
733 uniparental inheritance of mtDNA. *PeerJ*, 4:e2760, 2016.
- 734 [36] W. Handal, C. Szostek, N. Hold, M. Andrello, E. Thiébaud, E. Harney, G. Lefebvre, E.
735 Borcier, A. Jolivet, A. Nicolle, A. Boyé, E. Foucher, P. Boudry, and G. Charrier. New
736 insights on the population genetic structure of the great scallop (*Pecten maximus*) in the
737 English Channel, coupling microsatellite data and demogenetic simulations. *Aquatic*
738 *Conservation: Marine and Freshwater Ecosystems*, 30(10):1841–1853, 2020.
- 739 [37] G. M. Hewitt. Post-glacial re-colonization of european biota. *Biological journal of the*
740 *Linnean Society*, 68(1-2):87–112, 1999.
- 741 [38] T. J. Hilbish, F. P. Lima, P. M. Brannock, E. K. Fly, R. L. Rognstad, and D. S. Wethey.
742 Change and stasis in marine hybrid zones in response to climate warming. *Journal of*
743 *Biogeography*, 39(4):676–687, 2012.
- 744 [39] C. Hily. Redécouverte de *Macoma balthica* (Linnaeus, 1758) en rade de Brest. *An aod -*
745 *les cahiers naturalistes de l’Observatoire marin*, 2(1):31–35, 2013.
- 746 [40] R. D. Holt. On the evolutionary ecology of species’ ranges. *Evolutionary ecology*
747 *research*, 5(2):159–178, 2003.
- 748 [41] M. Huber. *Compendium of bivalves. A full-color guide to 3,300 of the world’s marine*
749 *bivalves. A status on Bivalvia after 250 years of research, volume 1.* ConchBooks,
750 Harxheim, 2010.
- 751 [42] M. Huber. *Compendium of bivalves. A full-color guide to the remaining seven families.*
752 *A systematic listing of 8’500 bivalve species and 10’500 synonyms, volume 2.*
753 ConchBooks, Harxheim, 2015.
- 754 [43] H. Hummel, R. Bogaards, T. Bek, L. Polishchuk, C. Amiard-Triquet, G. Bachelet, M.
755 Desprez, P. Strelkov, A. Sukhotin, A. Naumov, S. Dahle, S. Denisenko, M. Gantsevich,
756 K. Sokolov, and L. de Wolf. Sensitivity to stress in the bivalve *Macoma balthica* from

- 757 the most northern (Arctic) to the most southern (French) populations: low sensitivity in
758 Arctic populations because of genetic adaptations? *Hydrobiologia*, 355:127–138, 1997.
- 759 [44] M. T. Jolly, D. Jollivet, F. Gentil, E. Thiébaud, and F. Viard. Sharp genetic break
760 between Atlantic and English Channel populations of the polychaete *pectinaria koreni*,
761 along the north coast of France. *Heredity*, 94(1):23–32, 2005.
- 762 [45] M. T. Jolly, F. Viard, F. Gentil, E. Thiébaud, and D. Jollivet. Comparative
763 phylogeography of two coastal polychaete tubeworms in the Northeast Atlantic supports
764 shared history and vicariant events. *Molecular Ecology*, 15(7):1841–1855, 2006.
- 765 [46] M. Kearse, R. Moir, A. Wilson, S. Stones-Havas, M. Cheung, S. Sturrock, S. Buxton, A.
766 Cooper, S. Markowitz, C. Duran, T. Thierer, B. Ashton, P. Meintjes, and A. Drummond.
767 Geneious Basic: an integrated and extendable desktop software platform for the
768 organization and analysis of sequence data. *Bioinformatics*, 28(12):1647–1649, 2012.
- 769 [47] M. Kimura. A simple method for estimating evolutionary rate of base substitutions
770 through comparative studies of nucleotide sequences. *Journal of Molecular Evolution*,
771 16:111–120, 1980.
- 772 [48] R. Krebs. Combining paternally and maternally inherited mitochondrial DNA for
773 analysis of population structure in mussels. *Molecular Ecology*, 13:1701–1705, 2004.
- 774 [49] R. Krebs, W. Borden, N. Evans, and F. Doerder. Differences in population structure
775 estimated within maternally- and paternally-inherited forms of mitochondria in *Lampsilis*
776 *siliquoidea* (Bivalvia: Union-idae). *Biological Journal of the Linnean Society*, 109:229–
777 240, 2013.
- 778 [50] E. Ladoukakis, C. Saavedra, A. Magoulas, and E. Zouros. Mitochondrial DNA variation
779 in a species with two mitochondrial genomes: the case of *Mytilus galloprovincialis* from
780 the Atlantic, the Mediterranean and the Black Sea. *Molecular Ecology*, 11:755–769,
781 2002.
- 782 [51] P. Le Mao, L. Godet, J. Fournier, N. Desroy, F. Gentil, and E. Thiébaud. Mollusques. In
783 E. de la Station biologique de Roscoff, editor, *Atlas de la faune marine invertébrée du*
784 *golfe Normano-Breton*, volume 3/7, 2020.
- 785 [52] J. Leigh and D. Bryant. PopART: Full-feature software for haplotype network
786 construction. *Methods in Ecology and Evolution*, 6(9):1110–1116, 2015.
- 787 [53] P. Librado and J. Rozas. DnaSP v5: A software for comprehensive analysis of DNA
788 polymorphism data. *Bioinformatics*, 25:1451–1452, 2009.

- 789 [54] H.-P. Liu, J. B. Mitton, and S.-K. Wu. Paternal mitochondrial DNA differentiation far
790 exceeds maternal mitochondrial DNA and allozyme differentiation in the freshwater
791 mussel, *Anodonta grandis grandis*. *Evolution*, pages 952–957, 1996.
- 792 [55] P. Lubet, N. Devauchelle, M. Muzellec, Y. Paulet, R. Faveris, and J. Dao. Reproduction
793 of *Pecten maximus* from different fisheries areas Rade de Brest, Baie de St Brieuc, Baie
794 de Seine. In *Fisheries, Biology and Aquaculture of Pectinids*, 8th International Pectinid
795 Workshop, pages 22–29, Cherbourg (France), 1991.
- 796 [56] M. Lubosny, A. Przulucka, B. Smietanka, and A. Burzynski. *Semimytilus algosus*: first
797 known hermaphroditic mussel with doubly uniparental inheritance of mitochondrial
798 DNA. *Scientific Reports*, 10(1):1–12, 2020.
- 799 [57] P. C. Luttikhuisen, J. Drent, and A. Baker. Disjunct distribution of highly diverged
800 mitochondrial lineage clade and population subdivision in a marine bivalve with pelagic
801 larval dispersal. *Molecular Ecology*, 12:2215–2229, 2003.
- 802 [1] C. A. Maggs, R. Castilho, D. Foltz, C. Henzler, M. T. Jolly, J. Kelly, J. Olsen, K. E.
803 Perez, W. Stam, R. Vainölä, et al. Evaluating signatures of glacial refugia for North
804 Atlantic benthic marine taxa. *Ecology*, 89(sp11): S108–S122, 2008.
- 805 [58] G. M. Martin-Garcia. Oceanic impact on European climate changes during the
806 Quaternary. *Geosciences*, 9(3):119, 2019.
- 807 [59] J. McDonald and M. Kreitman. Adaptive protein evolution at the *Adh* locus in
808 *Drosophila*. *Nature*, 351:652–654, 1991.
- 809 [60] B. Meehan. A genetic comparison of *Macoma balthica* (Bivalvia: Telinidae) from the
810 eastern and western North Atlantic Ocean. *Marine Ecology Progress Series*, 28:69–76,
811 1985.
- 812 [61] L. Milani, F. Ghiselli, and M. Passamonti. Sex-linked mitochondrial behavior during
813 early embryo development in *Ruditapes philippinarum* (Bivalvia Veneridae) a species
814 with the doubly uniparental inheritance (DUI) of mitochondria. *Journal of Experimental*
815 *Zoology Part B: Molecular and Developmental Evolution*, 318(3):182–189, 2012.
- 816 [62] R. Nikula, P. Strelkov, and R. Vainölä. Diversity and trans-arctic invasion history of
817 mitochondrial lineages in the North Atlantic *Macoma balthica* complex (Bivalvia:
818 Tellinidae). *Evolution*, 61(4):928–941, 2007.
- 819 [63] R. Nikula, P. Strelkov, and R. Vainölä. A broad transition zone between an inner Baltic
820 hybrid swarm and a pure North Sea subspecies of *Macoma balthica* (Mollusca,
821 Bivalvia). *Molecular Ecology*, 17(6):1505–1522, 2008.

- 822 [64] B. S. Ort and G. H. Pogson. Molecular population genetics of the male and female
823 mitochondrial DNA molecules of the California sea mussel, *Mytilus californianus*.
824 *Genetics*, 177(2):1087–1099, 2007.
- 825 [65] E. Pante, V. Becquet, A. Viricel, and P. Garcia. Investigation of the molecular signatures
826 of selection on ATP synthase genes in the marine bivalve *Limecola balthica*. *Aquatic*
827 *Living Resources*, 32(3):7, 2019.
- 828 [66] E. Pante, C. Poitrimol, A. Saunier, V. Becquet, and P. Garcia. Putative sex-linked
829 heteroplasmy in the tellinid bivalve *Limecola balthica* (Linnaeus, 1758). *Journal of*
830 *Molluscan Studies*, 83(2):226–228, 2017.
- 831 [67] E. Pante, A. Rohfritsch, V. Becquet, K. Belkhir, N. Bierne, and P. Garcia. SNP detection
832 from De Novo transcriptome sequencing in the bivalve *Macoma balthica*: marker
833 development for evolutionary studies. *PLoS ONE*, 7(12):e52302, 2012.
- 834 [68] E. Paradis. pegas: an R package for population genetics with an integrated–modular
835 approach. *Bioinformatics*, 26(3):419–420, 2010.
- 836 [69] M. Passamonti. An unusual case of gender-associated mitochondrial DNA heteroplasmy:
837 the mytilid *Musculista senhousia* (Mollusca Bivalvia). *BMC Evolutionary Biology*,
838 7(Suppl 2)(S7), 2007.
- 839 [70] R. Pohlo. Evolution of the Tellinacea (Bivalvia). *Journal of Molluscan Studies*, 48:245–
840 256, 1982.
- 841 [71] E. Quemere, J.-L. Bagliniere, J.-M. Roussel, G. Evanno, P. McGinnity, and S. Launey.
842 Seascape and its effect on migratory life-history strategy influences gene flow among
843 coastal brown trout (*Salmo trutta*) populations in the English Channel. *Journal of*
844 *Biogeography*, 2016.
- 845 [72] R Core Team. R: A Language and Environment for Statistical Computing. R Foundation
846 for Statistical Computing, Vienna, Austria, 2020.
- 847 [73] P. D. Rawson and T. J. Hilbish. Evolutionary relationships among the male and female
848 mitochondrial DNA lineages in the *Mytilus edulis* species complex. *Molecular Biology*
849 *and Evolution*, 12(5):893–901, 1995.
- 850 [74] C. Riginos and C. W. Cunningham. Hybridization in postglacial marine habitats.
851 *Molecular Ecology*, 16(19):3971–3972, 2007.
- 852 [75] C. Riginos, M. J. Hickerson, C. M. Henzler, and C. W. Cunningham. Differential
853 patterns of male and female mtDNA exchange across the Atlantic Ocean in the blue
854 mussel, *Mytilus edulis*. *Evolution*, 58(11):2438–2451, 2004.

- 855 [76] T. Ruellet. Contribution à la dynamique de population de *Macoma balthica* en baie de
856 Somme dans le cadre du projet COMORES. Technical Report 13-027, Rapport du
857 GEMEL, 2013.
- 858 [77] C. Saavedra, D. T. Stewart, R. R. Stanwood, and E. Zouros. Species-specific segregation
859 of gender-associated mitochondrial DNA types in an area where two mussel species
860 (*Mytilus edulis* and *M. trossulus*) hybridize. *Genetics*, 143(3):1359–1367, 1996.
- 861 [78] A. Saunier. Bases génétiques de la différenciation adaptative en milieu anthropisé chez
862 *Macoma balthica*, un bivalve marin à fort flux génique. PhD thesis, Université de La
863 Rochelle, 2015.
- 864 [79] L. C. Shimmin, B. H.-J. Chang, and W.-H. Li. Male-driven evolution of DNA
865 sequences. *Nature*, 362(6422):745–747, 1993.
- 866 [80] D. Skibinski, C. Gallagher, and C. Beynon. Sex-limited mitochondrial DNA
867 transmission in the marine mussel *Mytilus edulis*. *Genetics*, 138(3):801–809, 1994.
- 868 [81] O. Skibinski, C. Gallaguer, and H. Quesada. On the roles of selection, mutation and drift
869 in the evolution of mitochondrial DNA diversity in British *Mytilus edulis* (Mytilidae;
870 Mollusca) populations. *Biological Journal of the Linnean Society*, 68:195–213, 1999.
- 871 [82] B. Smietanka and A. Burzynski. Disruption of doubly uniparental inheritance of
872 mitochondrial DNA associated with hybridization area of European *Mytilus edulis* and
873 *Mytilus trossulus* in Norway. *Marine Biology*, 164(11):209, 2017.
- 874 [83] B. Smietanka, A. Burzynski, and R. Wenne. Molecular population genetics of male and
875 female mitochondrial genomes in European mussels *Mytilus*. *Marine Biology*,
876 156(5):913–925, 2009.
- 877 [84] B. Smietanka, M. Zbawicka, T. Sanko, R. Wenne, and A. Burzynski. Molecular
878 population genetics of male and female mitochondrial genomes in subarctic *Mytilus*
879 *trossulus*. *Marine Biology*, 160(7):1709–1721, 2013.
- 880 [85] D. T. Stewart, E. R. Kenchington, R. K. Singh, and E. Zouros. Degree of selective
881 constraint as an explanation of the different rates of evolution of gender-specific
882 mitochondrial DNA lineages in the mussel *Mytilus*. *Genetics*, 143(3):1349–1357, 1996.
- 883 [86] D. T. Stewart, C. Saavedra, R. R. Stanwood, A. O. Ball, and E. Zouros. Male and female
884 mitochondrial DNA lineages in the blue mussel (*Mytilus edulis*) species group.
885 *Molecular Biology and Evolution*, 12(5):735–747, 1995.
- 886 [87] P. Strelkov, R. Nikula, and R. Väinölä. *Macoma balthica* in the White and Barents Seas:
887 properties of a widespread marine hybrid swarm (Mollusca: Bivalvia). *Molecular*
888 *Ecology*, 16(19):4110–4127, 2007.

- 889 [88] H. Stuckas, K. Stoof, H. Quesada, and R. Tiedemann. Evolutionary implications of
890 discordant clines across the Baltic *Mytilus* hybrid zone (*Mytilus edulis* and *Mytilus*
891 *trossulus*). *Heredity*, 103:146–156, 2009.
- 892 [89] F. Tajima. Evolutionary relationship of DNA sequences in finite populations. *Genetics*,
893 105(2):437–460, 1983.
- 894 [90] F. Tajima. Statistical method for testing the neutral mutation hypothesis by DNA
895 polymorphism. *Genetics*, 123(3):585–595, 1989.
- 896 [91] I. Theologidis, S. Fodelianakis, M. Gaspar, and E. Zouros. Doubly uniparental
897 inheritance (DUI) of mitochondria DNA in *Donax trunculus* (Bivalvia: Donacidae) and
898 the problem of its sporadic detection in Bivalvia. *Evolution*, 62(4):959–970, 2008.
- 899 [92] D. P. L. Toews and A. Brelsford. The biogeography of mitochondrial and nuclear
900 discordance in animals. *Molecular Ecology*, 21(16):3907–3930, 2012.
- 901 [93] R.-E. Trejo-Salazar, G. Castellanos-Morales, D. Hernandez-Rosales, N. Gamez, J.
902 Gasca-Pineda, M. R. M. Garza, R. Medellin, and L. E. Eguiarte. Discordance in maternal
903 and paternal genetic markers in lesser long-nosed bat *Leptonycteris yerbabuena*, a
904 migratory bat: recent expansion to the North and male phylopatry. *PeerJ*, 9:e12168,
905 2021.
- 906 [94] M. Turelli and L. C. Moyle. Asymmetric Postmating Isolation: Darwin’s Corollary to
907 Haldane’s Rule. *Genetics*, 176:1059–1088, 2007.
- 908 [95] R. Väinölä. Repeated trans-Arctic invasions in littoral bivalves: molecular zoogeography
909 of the *Macoma balthica* complex. *Marine Biology*, 143(5):935–946, 2003.
- 910 [96] E. Zouros. The exceptional mitochondrial DNA system of the mussel family Mytilidae.
911 *Genes & Genetic Systems*, 75(6):313–318, 2000.
- 912 [97] E. Zouros. Biparental inheritance through uniparental transmission: the doubly
913 uniparental inheritance (DUI) of mitochondrial DNA. *Evolutionary Biology*, 40:1–31,
914 2013.
- 915 [98] E. Zouros, A. O. Ball, C. Saavedra, and K. R. Freeman. An unusual type of
916 mitochondrial DNA inheritance in the blue mussel *Mytilus*. *Proceedings of the National*
917 *Academy of Sciences*, 91(16):7463–7467, 1994.
- 918
- 919

920 **Legends**

921 Figure 1: Median joining networks constructed from the haplotypes found among the 313
922 individuals distributed in 17 sampling sites for (A) the *cox1f* gene (479bp) and (C) the
923 *cox1m-long* gene (676bp). Haplotype associations among haplogroups are represented with a
924 tanglegram (B) with bold lines highlighting individuals sharing distant haplogroups

925

926 Figure 2: Geographical distribution of the *cox1f* and *cox1m-long* haplogroups: haplogroup
927 frequencies are represented for each marker in all the sites with a pie chart. The size of the
928 pie chart indicates the number of individuals analyzed.

929

930 Figure 3: Heatmap representing linkage disequilibrium among haplogroups of *cox1f* and
931 *cox1m-long*. Color key is based on correlation values among haplogroups and cell value
932 represent the observed frequencies of each possible association. Dendrogram based on
933 pairwise distance between main haplotypes of each haplogroup using the Tamura-Nei
934 nucleotide substitution model and a gamma correction of 0.1150 and 0.1450 for *cox1f* and
935 *cox1m-long* respectively.

936

937 Figure 4: Bayesian skyline plots for North and South subpopulations illustrating effective
938 population size (N_e) variation through time for both markers. The lines represent the mean
939 effective population size, and the colored area represent 95% higher and lower confidence
940 interval of posterior probabilities Here the 90 My divergence time with the *Donax* genus is
941 considered (5.19×10^{-2} substitution/site/My).

942

943 Figure 5: Comparison of pairwise Φ_{ST} estimated at the *cox1f* gene between common sampling
944 sites studied in Becquet et al (2012) (males and females) and the present study (males only).
945 The plain line represents the $x=y$ axis and the dash line, the linear regression ($y = 1.27 x +$
946 0.03 , $df = 62$, $R^2_{adj}=0.74$, $p<0.001$). A Mantel test revealed a significant correlation between
947 the two datasets ($r=0.786$, $p=0.0084$).

948

949

950

951 Table 1: Genetic diversity indices at *cox1f* (479bp) and *cox1m* (479bp) loci for each sampling
952 site: n: number of individuals, nsites: number of polymorphic sites, H: number of haplotypes,
953 π : nucleotide diversity, Hd: Haplotype diversity and D: Tajima's D coefficient. N_{eF}/N_{eM} : the
954 ratio of female to male effective population size * indicates significant values (<0.05 , 10000
955 permutations), Na: not available

Geographic zone	Sampling site	n	<i>cox1f</i>				<i>cox1m</i>					N _{ef} /N _{eM}	
			nsites	H	$\pi(10^2)$	Hd	D	nsites	H	$\pi(10^2)$	Hd		D
North	Umea (UME)	2	6	2	1.41	-	-	12	2	2.5	-	-	-
	Lomma (LOM)	6	7	3	0.81	-	-	4	3	0.28	-	-	-
	Mecklenburg bight (MEC)	3	4	3	0.61	-	-	10	3	1	-	-	-
	Sylt (SYL)	7	7	4	0.91	-	-	5	4	0.38	-	-	-
	Wilhelmshaven (WIL)	3	0	1	0.00	-	-	1	3	0.13	-	-	-
	Crildumersiel (CRI)	10	6	2	0.77	0.53	2.10	14	9	0.70	0.98	-1.47	0.04
	Kruiningen (KRU)	22	11	7	0.77	0.69	0.11	10	22	0.23	0.65	-2.00*	2.30
<i>all</i>	42	11	7	0.75±0.43	0.64±0.06	0.75	23	16	0.36±0.24	0.79±0.05	-2.26*	0.91	
Center	Le Crotoy (CRO)	28	13	7	0.77	0.58	-0.24	14	14	0.38	0.88	-1.68*	0.36
	Saint Vaast (VAA)	31	11	5	0.33	0.24	-1.63*	11	9	0.27	0.75	-1.69*	0.29
	<i>all</i>	59	14	9	0.52±0.31	0.42±0.08	-0.79	20	20	0.32±0.21	0.81±0.04	-1.99*	0.33
Hybrid/Finistère	Mont Saint Michel (MSM)	31	8	4	0.22	0.24	-1.60*	5	7	0.11	0.35	-1.51*	1.11
	Saint Brieuc (BRI)	30	15	9	0.76	0.99	0.17	4	5	0.08	0.36	-1.58*	337.1
	<i>all</i>	61	16	10	0.74±0.42	0.58±0.07	-0.28	8	10	0.09±0.09	0.35±0.08	-1.91*	4.9
South	Pont Mahé (MAH)	30	8	6	0.18	0.36	-1.86*	5	6	0.07	0.31	-2.00*	2.4
	Saint Brevin (BRE)	29	9	8	0.71	0.49	-0.25	8	9	0.13	0.53	-2.14*	1.6
	Noirmoutier (NOI)	8	3	4	0.23	-	-	1	2	0.05	-	-	-
	Aytré (AYT)	33	8	6	0.43	0.55	-0.18	5	6	0.07	0.28	-1.88*	6.0
	Fouras (FOU)	30	8	7	0.29	0.50	-1.12	6	6	0.08	0.31	-2.10*	4.2
	<i>all</i>	63	11	10	0.36±0.23	0.52±0.07	-0.89	9	9	0.08±0.08	0.29±0.07	-2.15*	5.09
	Arcachon (ARC)	10	5	3	0.23	0.38	-1.74*	1	2	0.04	0.2	-1.11	4.70
All	313	37	37	0.85	0.76	-1.13	55	64	0.42	0.70	-2.28*	2.60	

bioRxiv preprint doi: <https://doi.org/10.1101/2022.02.28.479517>; this version posted March 2, 2022. The copyright holder for this preprint (which was not certified by peer review) is the author/funder, who has granted bioRxiv a license to display the preprint in perpetuity. It is made available under aCC-BY-NC-ND 4.0 International license.

958

959 Table 2: Analysis of molecular variance (AMOVA) to partition the genetic variation among hierarchical geographical scales. Results are
 960 presented for both markers, with different options of hierarchical grouping of subpopulations.
 961

Number of groups	Groups		<i>coxIf</i>			<i>CoxIm</i>		
			Among groups relative to total variance	Among subpopulations within groups	Among subpopulations relative to total variance	Among groups relative to total variance	Among subpopulations within groups	Among subpopulations relative to total variance
3	(CRI,KRU) (CRO,VAA,MSM,BRI) (MAH,BRE,AYT,FOU,ARC)	% var	44.71	7	48.29	22.2	22.54	55.26
		Fixation indices	$\Phi_{CT}=0.447^{***}$	$\Phi_{SC}=0.517^{***}$	$\Phi_{ST}=0.126^{**}$	$\Phi_{CT}=0.221^{ns}$	$\Phi_{SC}=0.290^{***}$	$\Phi_{ST}=0.447^{***}$
2	(CRI,KRU,CRO,VAA) (MSM,BRI,MAH,BRE,AYT,FOU,ARC)	% var	16.98	31.02	52	57.36	0.56	42.08
		Fixation indices	$\Phi_{CT}=0.170^{ns}$	$\Phi_{SC}=0.374^{***}$	$\Phi_{ST}=0.480^{***}$	$\Phi_{CT}=0.574^{***}$	$\Phi_{SC}=0.013^{ns}$	$\Phi_{ST}=0.579^{***}$
2	(CRI,KRU,CRO,VAA,MSM,BRI) (MAH,BRE,AYT,FOU,ARC)	% var	49.14	6.4	44.46	21.88	4.18	53.94
		Fixation indices	$\Phi_{CT}=0.491^{***}$	$\Phi_{SC}=0.126^{***}$	$\Phi_{ST}=0.555^{**}$	$\Phi_{CT}=0.212^*$	$\Phi_{SC}=0.309^{***}$	$\Phi_{ST}=0.460^{**}$

962 *P>0.05, **P>0.01, ***P < 0.001, ns: non significant

963

964

965 Table 3: McDonald and Kreitman contingency table: the number of non-synonymous and
 966 synonymous substitutions within and among mitotypes for the two *L. balthica* genetic
 967 lineages, the neutrality index (NI) and the results from the Fisher Exact and G tests.

968

969

Group	<i>coxIf</i> vs. <i>coxIm</i> segregating sites	Polymorphic	Fixed	NI	Fisher Exact Test	
					Pvalue	G test
North						
	Non-synonymous	2	56	0.083	<0.0001	20.165***
	Synonymous	32	74			
South						
	Non-synonymous	2	54	0.107	<0.0002	15.111***
	Synonymous	29	84			

970 ***P < 0.0001,

971

972 Table 4: Measures of nonsynonymous to synonymous (i) nucleotide diversity
 973 within each mitotype (π_a , π_s) and (ii) number of substitutions among mitotypes (K_a , K_s) using
 974 the Jukes and Cantor correction

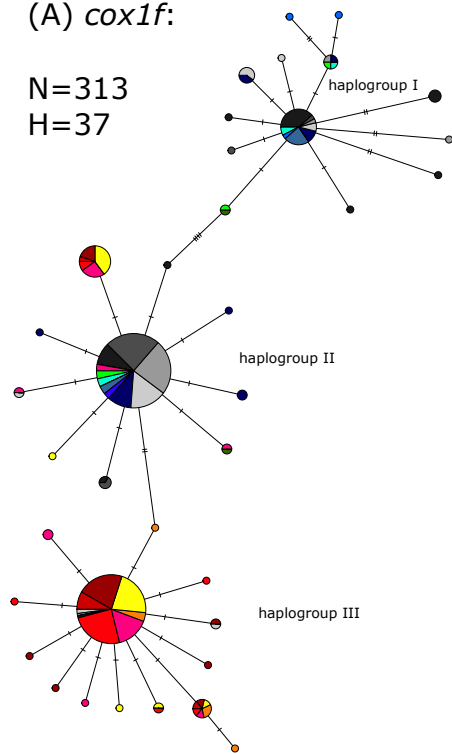
		Intra mitotype (10^2)			Inter-mitotype		
		π_a	π_s	ratio	K_a	K_s	ratio
North	f	0.000	2.779	0.000	0.201	2.008	0.100±0.028
	m	0.026	1.401	0.018			
South	f	0.011	1.421	0.008	0.201	2.086	0.097±0.031
	m	0.005	0.348	0.015			
All	f	0.008	2.733	0.003	0.201	2.063	0.098±0.029
	m	0.012	1.037	0.011			

975

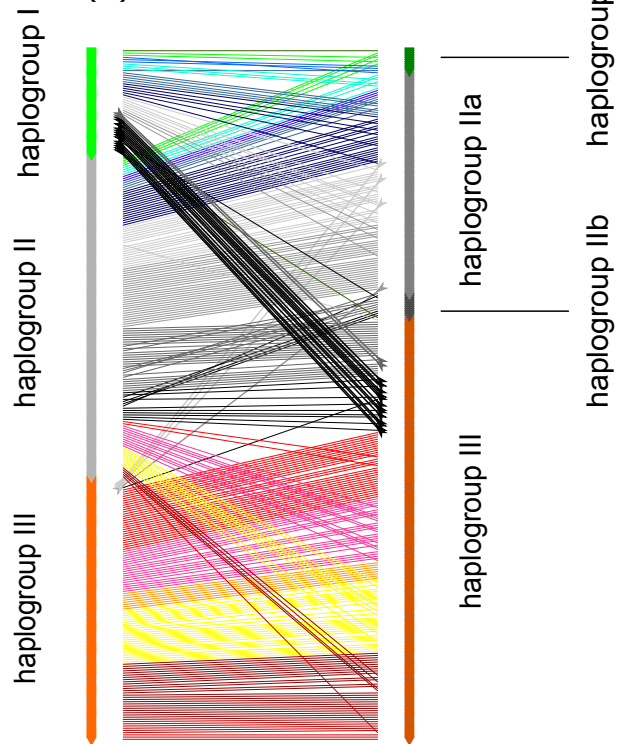
(A) *cox1f*:

N=313

H=37



(B)



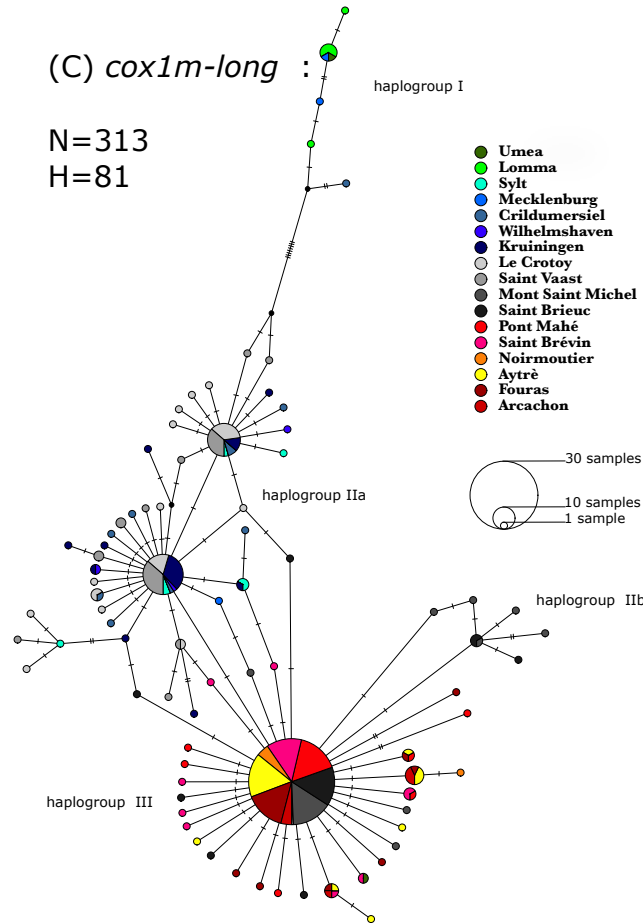
cox1f

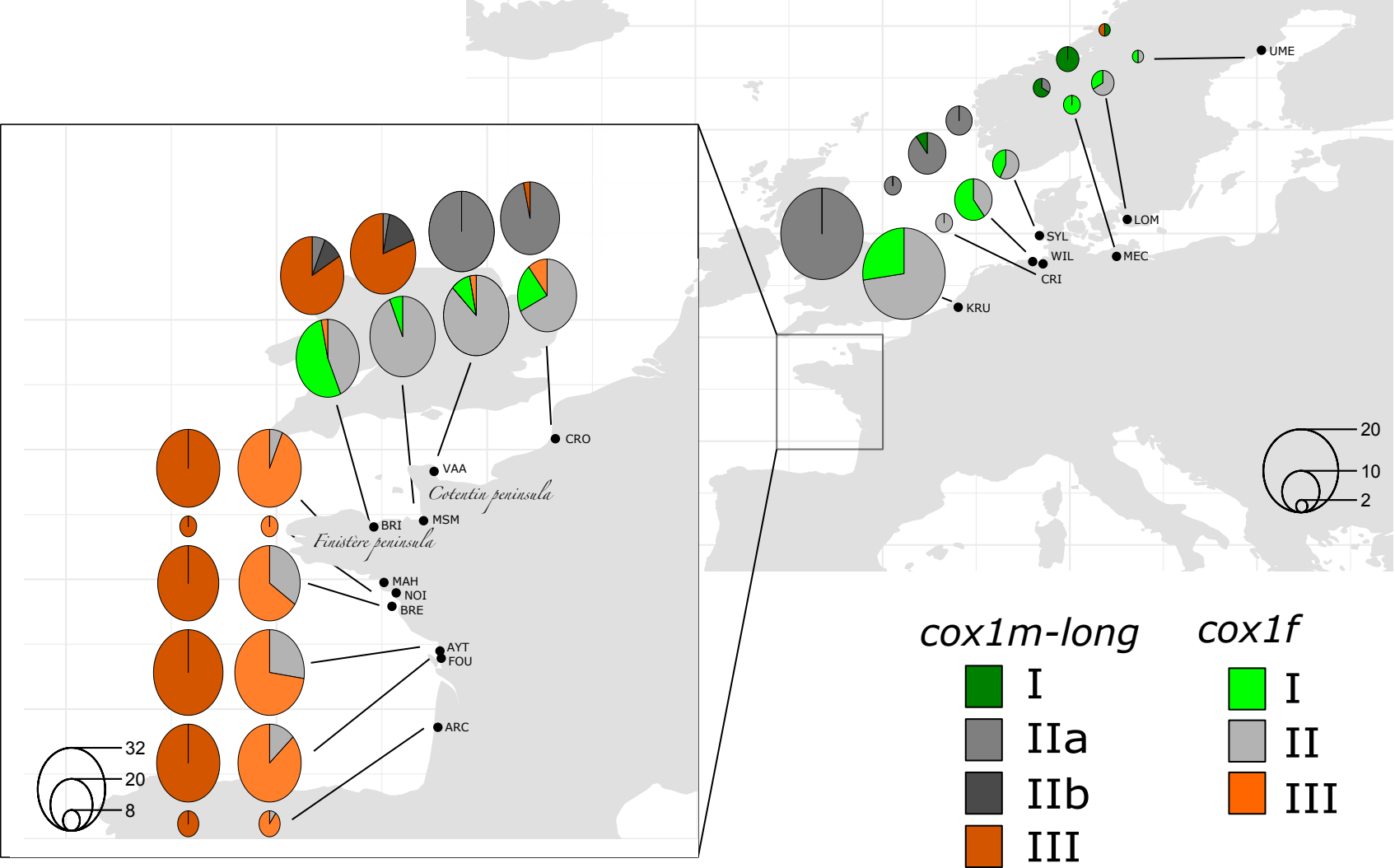
cox1m-long

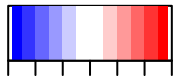
(C) *cox1m-long* :

N=313

H=81







-0.6 0 0.4

Correlations among haplotypes

